Phase diagram of the Kondo necklace: a mean-field renormalization group approach

2001 J. Phys. A: Math. Gen. 34 10829

(http://iopscience.iop.org/0305-4470/34/49/306)

INSTITUTE OF PHYSICS PUBLISHING JOURNAL OF PHYSICS A: MATHEMATICAL AND GENERAL

J. Phys. A: Math. Gen. **34** (2001) 10829–10837 PII: S0305-4470(01)25476-6

Phase diagram of the Kondo necklace: a mean-field renormalization group approach

Tatiana G Rappoport and M A Continentino

Instituto de Física, Universidade Federal Fluminense, CEP 24210-340, Niteroi RJ, Brazil

E-mail: tatiana@if.uff.br

Received 1 June 2001, in final form 18 September 2001
Published 30 November 2001
Online at stacks.iop.org/JPhysA/34/10829

Abstract

In this paper we investigate the magnetic properties of heavy fermions in the antiferromagnetic and dense Kondo phases in the framework of the Kondo necklace model. We use a mean-field renormalization group approach to obtain a temperature versus Kondo coupling (T–J) phase diagram for this model in qualitative agreement with Doniach's diagram, proposed on physical grounds. We further analyse the magnetically disordered phase using a two-site approach. We calculate the correlation functions and the magnetic susceptibility that allow us to identify the crossover between the spin-liquid and the local moment regimes, which occurs at a *coherence* temperature.

PACS numbers: 75.30.Mb, 05.50.+q, 75.20.Hr

1. Introduction

It is well known that the nature of the ground state of the dense Kondo compounds results basically from the competition between the Ruderman–Kittel–Kasuya–Yosida (RKKY) interaction and the Kondo effect. In a simple picture it is governed by a single parameter, the ratio J/W, where J is the effective exchange between localized moments and conduction electrons and W is the bandwidth of the latter. The value of this ratio is usually tunable experimentally by pressure or composition ratio of the compounds. The RKKY interaction is an indirect magnetic interaction between localized moments, mediated by the polarized conduction electrons, with an energy scale of order $J_{\mathrm{RKKY}} \propto \frac{J^2}{W}$, which produces a long-range ordered magnetic ground state. On the other hand, the Kondo effect favours the formation of singlet states between localized moments and conduction electrons generating a non-magnetic ground state and, in the single impurity case, has a characteristic energy scale of the order $k_B T_K = W\mathrm{e}^{-W/J}$. As a result of the interplay between these two effects, some Kondo compounds are non-magnetic and are characterized by a heavy-fermion behaviour (Fermi-liquid) at very low temperatures, while others order magnetically, generally

antiferromagnetically. The study of this interplay is easily formulated using the Kondo lattice model (KLM), which emphasizes the importance of spin fluctuations neglecting charge fluctuations of the localized electrons and has been well characterized by the 'Doniach phase diagram' [1]. In a simple picture, the ordering temperature T_N initially increases with increasing J, then passes through a maximum and vanishes at a critical coupling J_c. At this quantum critical point (QCP), a second-order phase transition between an antiferromagnetic ground state for small values of J and a dense Kondo state for strong couplings J occurs. This behaviour of T_N has been experimentally observed in many cerium compounds by varying the pressure applied to the system [2–4] or the relative concentration in the compounds [5, 6]. Many theoretical studies have been done in order to study the phase diagram [7–11], the nature of this critical point [12] as well as the effect of the disorder introduced by pressure and substitutions in the Kondo lattice systems [13–15].

In this paper we are interested in studying the T–J phase diagram of the Kondo compounds. For this purpose, we use an analogue of the symmetric Kondo lattice with the complete absence of charge fluctuations the Kondo necklace model (KNM). This model was proposed by Doniach [1] and its ground state has been investigated by a variety of methods [16–20]. In order to assess the critical behaviour of the Kondo necklace, we apply the mean-field renormalization group (MFRG), first proposed by Indekeu *et al* [21], on the KNM. This method combines mean field results for small clusters of spins and renormalization group ideas. While mean-field theory identifies the order parameter of the cluster with the order parameter of the entire system, the MFRG assumes that the cluster order parameter rescales with cluster size [22]. Using this method we obtain the phase diagram of the Kondo necklace as a function of temperature and Kondo coupling, which is qualitatively identical to the Doniach diagram. Within a two-site approach [23], we calculate the finite temperature magnetic susceptibility and investigate the behaviour of short-range magnetic correlations in the magnetically disordered phase. As a result of this investigation, we increase the phase diagram with a crossover line, which is associated with a coherence temperature that separates Kondo spin-liquid and localized moments regimes.

This paper is organized as follows: in the next section we present the Kondo lattice and Kondo necklace models and discuss their analogies. In section 3 we apply the MFRG approach in the KNM and obtain the Doniach phase diagram, which we compare with experimental results. In section 4 we apply a two-site method on the non-magnetic phase in order to study the role of short-range correlations on the system. We also calculate the magnetic susceptibility and then obtain a coherence temperature. In section 5 we summarize and discuss our results.

2. The model

The KLM is a theoretical model for heavy fermions that can be derived from the more fundamental Anderson lattice model in the case of well-developed local spin moments [24]. It consists of two different types of electrons, the localized spins whose charge degrees of freedom are suppressed and the conduction electrons that propagate as charge carriers. It is described by

$$H = -t \sum_{\langle i,j \rangle} (c^{\dagger}_{i,\sigma} c_{j,\sigma} + \text{h.c.}) + J \sum_{i} \mathbf{S}_i \cdot c^{\dagger}_{i,\alpha} \boldsymbol{\sigma}_{\alpha\beta} c_{i,\beta}. \tag{1}$$

The first term represents the conduction band ($c^{\dagger}_{i,\sigma}$ is the creation operator, t is the hopping between nearest neighbours) and the second term is the interaction between conduction

electrons and localized moments $\mathbf{S}_i$ via the intra-site exchange J, where σ are the Pauli matrices.

In order to study the interplay between Kondo screening and the RKKY interaction, Doniach proposed a simplified model related to the one-dimensional Kondo lattice, called the KNM. In this model, the conduction electrons are replaced by a spin chain with XY coupling which eliminates charge fluctuations [1]:

$$H_{\mathrm{KN}} = W \sum_{\langle i,j \rangle} \left(\tau_i^x \tau_j^x + \tau_i^y \tau_j^y \right) + J \sum_i \mathbf{S}_i \cdot \boldsymbol{\tau}_i \tag{2}$$

where τ_i and $\mathbf{S}_i$ are independent sets of spin-1/2 Pauli operators. The first term mimics electron propagation and in one dimension can be mapped by the Jordan–Wigner transformation onto a band of spinless fermions. The second term is the magnetic interaction between conduction electrons and localized spins $\mathbf{S}_i$ via the coupling J, as in equation (1).

Although the KLM is mapped onto the KNM only in one dimension, it is clear that, even in higher dimensions, H_{KN} has the same magnetic tendencies of the Kondo lattice. Since the essential features of the original model are kept, we expect that the main physical properties of the Kondo lattice will be maintained in the model described by equation (2).

Since in the KNM approach to the Kondo lattice charge fluctuations are neglected, the critical properties in this case are described just by spin excitations. However, it is important to emphasize that the analysis of heavy fermion systems in terms of the KNM is appropriate [27]. A recent and very complete study of a heavy fermion system just at the QCP [28] shows that a description in terms of local moments seems to be more appropriate for this kind of material. This may not be the case for all heavy fermions but it is also true that the universality class of the quantum transition of heavy fermions has not been determined yet and may even not be unique.

3. Mean-field renormalization group

The mean-field renormalization group was first proposed by Indekeu *et al* [21] for computing critical properties of lattice spin systems. This method has been applied to many statistical problems of physics, both classical and quantum systems, with [25] and without disorder [21] and the resulting critical exponents deviate from those obtained from standard mean-field theories (including Bethe lattice calculations) [22].

The main idea of the MFRG is the comparison of two clusters with N and N' sites, respectively, subject to symmetry-breaking boundary conditions. The interactions within the clusters are treated exactly, and the effect of the surrounding sites is replaced by a mean-field which is supposed to scale in the same way as the order parameter.

For a generic spin system, one considers each boundary spin fixed and equal to b and b' for the N and N' spin clusters respectively. After computing the order parameters $\mathcal{O}_N$ and $\mathcal{O}_{N'}$ for both the clusters, one imposes a scaling relation between them

$$\mathcal{O}_{N'}(K', b') = \xi \mathcal{O}_N(K, b) \tag{3}$$

with K and K' being the coupling constants of the two rescaled systems. Assuming a similar relation between the mean fields ($b' = \xi b$) and knowing that these fields have to be very small near the second-order phase transition, one can expand equation (3) for small values of b and b' to obtain

$$\left. \frac{\partial \mathcal{O}'_N(K', b')}{\partial b'} \right|_{b'=0} = \left. \frac{\partial \mathcal{O}_N(K, b)}{\partial b} \right|_{b=0} \tag{4}$$

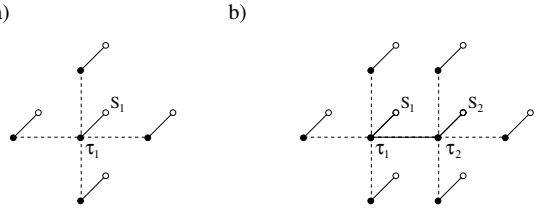

Figure 1. Clusters considered in the calculations of the two-dimensional case. Each site contains two spins, one spin S (open circle) connected by a solid line to one spin τ (filled circle). The interaction between the sites is mediated by the spins τ, where the dashed bonds represent the interactions with the boundary symmetry-breaking fields b' and b.

which is independent of the scaling factor ξ. Equation (4) can be interpreted as a recursion relation for the coupling constant K, from which the critical point K_c is extracted.

We can apply this method to the Kondo necklace in its simplest version, i.e., we consider two cells containing one and two sites each, as sketched in figure 1 for a two-dimensional hypercubic lattice.

As we deal with an incipient antiferromagnetic ordering and antiferromagnetism in the Kondo necklace occurs in the XY plane [1], we consider a D-dimensional hypercubic lattice and divide the system into two sub-lattices A and B. The order parameter is then the staggered magnetization of the spins τ, taken along the x-direction (see equations (5) and (6)). The x-component of the boundary spins in the smallest cluster is fixed to be $-b'$ since all the first neighbours of τ_1 are in the same sub-lattice. In the two-site cluster, τ_1 and τ_2 are in different sub-lattices, so the x-component of their neighbouring boundary spins has different signs and is fixed at $-b$ and b, respectively.

Let us first consider the Hamiltonian for a one-site cluster taken on a sub-lattice A,

$$H_1 = J'\mathbf{S}_1 \cdot \tau_1 - zb'W'\tau_1^x \tag{5}$$

where J' is the scaled coupling interaction and the spin τ_1 interacts with its z nearest neighbours through the term $zb'W'\tau_1^x$.

Similarly, the Hamiltonian for the two-site system (one in each sub-lattice) is given by

$$H_{12} = J\sum_{i=1}^{2}\mathbf{S}_i \cdot \tau_i + W\left(\tau_1^x\tau_2^x\right) - (z-1)bW\left(\tau_1^x - \tau_2^x\right). \tag{6}$$

In this case the spin τ_1 interacts directly with τ_2 through a term $W\left(\tau_1^x\tau_2^x\right)$ and both τ_1 and τ_2 interact with their $(z-1)$ nearest neighbours through $-(z-1)bW\tau_1^x$ and $(z-1)bW\tau_2^x$ respectively.

This method can be used to study quantum systems ($T = 0$), for which there are few available renormalization group techniques. For this purpose, we compute the ground states $|0\rangle_1$ and $|0\rangle_{12}$ of the two systems and their corresponding staggered magnetizations along the x-direction. In the vicinity of the phase transition, b and b' can be assumed to be small and

$$M_1^s = \langle 0|\tau_1^x|0\rangle = -\frac{z}{2j'}b'$$

$$M_{12}^s = \frac{\langle 0|\left(\tau_1^x - \tau_2^x\right)|0\rangle}{2} = -\frac{2\,(z-1)\,(\sqrt{16\,j^2+1}+1)^2}{(1+16\,j^2+\sqrt{16\,j^2+1})\,(-1+\sqrt{16\,j^2+1})}b$$

where $j = \frac{J}{W}$ and $j' = \frac{J'}{W'}$.

The main assumption of the MFRG is the imposition of the same scaling relations between M_1^s and M_{12}^s, b and b'. By doing this, we arrive at the renormalization group recursion relation for j and j'. The associated fixed point equation is

$$\frac{z}{j_c} = \frac{4(z-1)\left(\sqrt{16\,j_c^2+1}+1\right)^2}{\left(1+16\,j_c^2+\sqrt{16\,j_c^2+1}\right)\left(-1+\sqrt{16\,j_c^2+1}\right)}. \tag{7}$$

By solving equation (7) we obtain the antiferromagnetic QCP in any space of dimension D. For $z = 2$, which corresponds to a one-dimensional system, we obtained $j_c = 0.64$. The critical ratios j_c for other coordination numbers are $z = 4 \rightarrow j_c = 1.66$, $z = 6 \rightarrow j_c = 2.67$. These values can be compared with the recent results [20, 34] and the relative errors are 12.67% for the two-dimensional and 1.5% for three-dimensional showing that the results are most reliable for higher dimensions.

It is worth mentioning that the diagonalization of H_{12} is not a simple task. However, as we are interested in the small values of the mean field, a perturbative expansion can be worked out in order to obtain the eigenvalues and eigenvectors in powers of b [26]. We follow the same prescription in order to calculate the staggered magnetizations for $T \neq 0$.

As we have more than one variable, we cannot determine a complete renormalization flow in the $[j, T]$ plane. However, for a fixed j we can calculate T_N or vice versa. In order to obtain the critical values, we consider the solutions of the fixed point equation associated with equation (4), i.e.,

$$\left.\frac{\partial M_1^s(T_N, j)}{\partial b'}\right|_{b'=0} = \left.\frac{\partial M_{12}^s(T_N, j)}{\partial b}\right|_{b=0} \tag{8}$$

where for each $j < j_c$ we obtain a $T_N(j)$ and the set of all critical points yields the temperature-dependent phase diagram of the Kondo necklace. The critical line for a three-dimensional system ($z = 6$), is depicted in figure 2. Close to the zero temperature fixed point it behaves as

$$|\delta| = |j - j_c| \propto \mathrm{e}^{-\alpha(z, j_c)\beta_N} \qquad \beta_N = \frac{1}{k_B T_N}. \tag{9}$$

This dependence is characteristic of this approach and appears for any dimension.

Endstra *et al* [29] calculated the J couplings of many cerium and uranium compounds based fundamentally on the atomic radii and interatomic distances of these systems. More recently, Cornelius and Schilling, based on the variation of the lattice parameters generated by pressure and substitution of Si by Ge (negative pressure) in $CeM_2Si_{2-x}Ge_x$ compounds (where M = Rh, Ru, Pd) [30–32], found a relation between the Neèl temperature T_N and the coupling J for $CeRu_2Si_2$, $CeRh_2Si_2$ and $CePd_2Si_2$ [33]. Their results fall in Doniach-like curves, which when normalized by the maximum of T_N ($T_{\max}$) and its equivalent $J_{T_{\max}}$ collapse onto a single universal curve.

We observe that in the experimental results, the Neèl temperature becomes zero in the weak coupling regime at a value of J greater than zero, differently from the theoretical predictions for the Kondo lattice. By shifting the experimental results along the J-axis in order to obtain $T_N = 0$ at $J = 0$, and using the same normalization used in [33], we obtain the results of figure 3 ($z = 6$ (three-dimensional)), where one can see that the behaviour of the theoretical curve is in good agreement with the experimental values. We can conclude that these Kondo systems behave qualitatively as proposed by Doniach although in practice the long-range magnetic order vanishes before the theoretical $J = 0$ value is attained.

As we are dealing with a mean-field-like approach using small clusters we do not obtain a precise value for the QCP for a one-dimension case ($J = 0$) such as in previous studies [17–20]. Nevertheless, this method has the advantage of being very simple to implement at

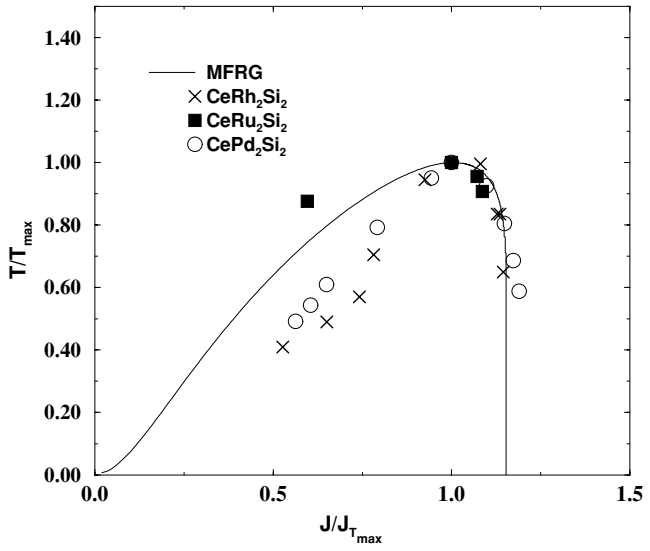

Figure 2. Phase diagram of the KNM within the mean-field renormalization group approach (with $z = 6$) compared with the experimental results for cerium compounds extracted from [33]. The results are normalized by the maximum value of the Neèl temperature T_N and its associated coupling J.

finite temperature and produce reliable values of the QCP for higher dimensions, as discussed before.

The main feature of the MFRG method in its simplest approach (one- and two-site cells) is that it yields the $[T, j]$ phase diagram for heavy fermions as proposed by Doniach on physical grounds [1]. This is so because this method captures the essential physics of the Kondo lattice problem, namely, the competition between the RKKY and Kondo interactions. However, it is important to note that the present method can be applied to larger clusters, which provides better information concerning the lattice topology of the system [22] in order to obtain more accurate values for the QCP for lower dimensions.

4. Short-range correlations

In the magnetically disordered phase, where the mean fields b and b' are identically zero, we can still calculate some properties of the system by means of a two-site approximation. This method consists in solving exactly a Hamiltonian of two sites, i.e., equation (6) with $b = 0$. As this finite size system does not present long-range (magnetic) order, we expect that this approach will unravel some aspects of the non-magnetic phase. For consistency of the analysis we shift j by the critical value j_c obtained previously such that the correlations in the dimers vanish at the QCP and not at $j = 0$. The analysis below is consequently valid not too close to the QCP in the region where the correlation length has not grown much beyond two atomic distances.

We can investigate the behaviour of short-range magnetic correlations as well as the intra-site correlations between localized moments and conduction electrons, which are related to the Kondo effect.

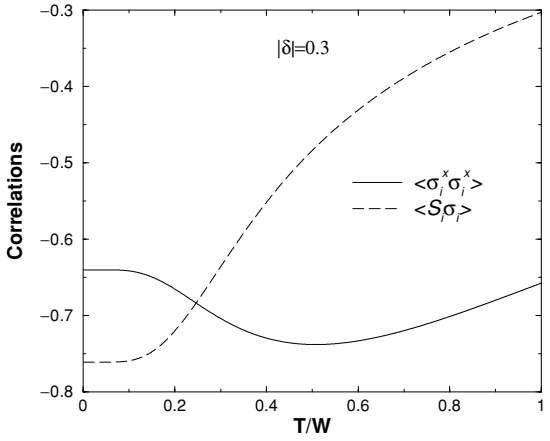

Figure 3. Competition between two kinds of correlation: the intra-site $\langle S \cdot \tau \rangle$ (dashed line) and the inter-site $\langle \tau_1^x \tau_2^x \rangle$ (solid line) for $|\delta| = 0.3$.

The localized–delocalized spin correlation function $\langle S \cdot \tau \rangle$ characterizes the condensation of singlet states. At $T = 0$, this function decreases for increasing values of j, saturating at the value -3, which is consistent with the strong coupling limit [19] where the system condenses into independent singlets at each site. As the temperature rises, this correlation rapidly falls to zero and we observe that, since coherence in the KNM is a collective phenomenon, even low-temperature excitations can destroy the Kondo spin-liquid regime. The inter-site correlation function $\langle \tau_1^x \tau_2^x \rangle$ represents the short-range magnetic correlations. This function has a minimum at a low temperature and then gradually vanishes as T increases. Differently from $\langle S \cdot \tau \rangle$, it has a smooth behaviour for large T and its asymptotic behaviour is independent of $|\delta| = |j - j_c|$.

The competition between these two kinds of correlations produces a change in the behaviour of the system, as illustrated in figure 3. For low temperatures, the correlation $\langle S \cdot \tau \rangle$ is stronger and the system is in a condensate of singlets, typical of the Kondo spin-liquid regime [20]. Near the minimum of the magnetic correlation function $\langle \tau_1^x \tau_2^x \rangle$ there is a crossover: $\langle \tau_1^x \tau_2^x \rangle$ begins to dominate and destroys these singlet states giving rise to a paramagnetic regime with localized moments. The inflection point in the magnetic correlation function, where it crosses $\langle S \cdot \tau \rangle$, defines the crossover or coherence temperature T_{coh} which separates the two different regimes in the non-magnetic region of the phase diagram.

The magnetic susceptibility (figure 4), calculated according to equation (10), illustrates the difference between these two regimes.

$$\chi_0 = Z^{-1} N^{-1} \beta \sum_m \mathrm{e}^{-\beta E_m} \left(M^x_{\mathrm{total}} \right)^2$$
$$Z = \sum_m \mathrm{e}^{-\beta E_m} \qquad \beta = \frac{1}{k_B T}. \tag{10}$$

At low temperatures ($T \ll T_{\mathrm{coh}}$), as we are dealing with the symmetric case of the Kondo lattice, the system is an insulator and there is a singlet–triplet gap. At a higher temperature there is a maximum in the susceptibility where the gap closes and finally, at high T ($T \gg T_{\mathrm{coh}}$), we can see an asymptotic Curie–Weiss regime, typical of localized moments.

The coherence temperature is calculated by finding the zero of $\frac{\partial^2 \langle \tau_1^x \tau_2^x \rangle}{\partial T^2}$. The Doniach diagram discussed in the previous section can be generalized in order to include two other

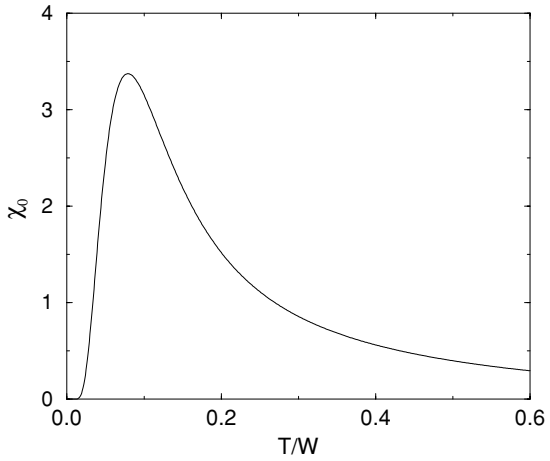

Figure 4. Magnetic susceptibility versus temperature for $|\delta| = 0.3$ obtained within the two-site approach.

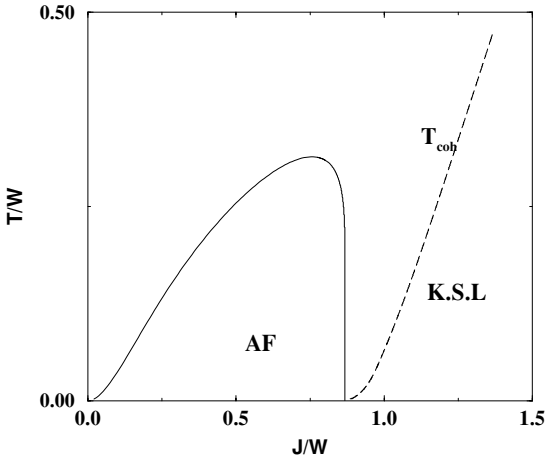

Figure 5. Complete phase diagram of the KNM (for $z = 6$). The curve $T_N(J)$ is shown here as a full line, whereas the dashed line represents $T_{\rm coh}(J)$.

regimes in the magnetically disordered region of the phase diagram, separated by the coherence line. figure 5 illustrates the extended diagram obtained by using these two methods.

5. Conclusions

We have successfully applied the MFRG on the KNM. Using the simplest choice of clusters, we obtained the quantum critical point for the two- and three-dimentional cases that are in good agreement with the previous calculations. We obtained for the first time a theoretical calculation of the Doniach diagram for the KNM and compared it with the experimental results for some cerium compounds obtaining qualitatively good agreement. In the magnetic disordered phase we calculated, using a two-site method, the short-range magnetic correlation function, the localized–delocalized spin correlation function as well as the magnetic susceptibility as a function of temperature and characterized two well-defined regimes: at low temperatures, a condensate of singlets with a singlet–triplet gap and at high

temperatures, a Curie–Weiss regime. The crossover line close to the QCP has been analytically calculated and presents a power-law behaviour.

Acknowledgments

The authors thank the Brazilian agencies CNPq and FAPERJ for financial support and Dr E Miranda for useful discussions at the initial stage of this study.

References

[1] Doniach S 1977 *Physica* B **91** 231
[2] Croft M C, Guertin R P, Kupferberg L C and Parks R D 1979 *Phys. Rev.* B **86-88** 177
[3] Eiling A and Schilling J S 1981 *Phys. Rev. Lett.* **46** 364
[4] Graf T, Thompson J D, Hundley M F, Movshovich R, Fisk Z, Mandrus D, Fisher R A and Phillips N E 1997 *Phys. Rev. Lett.* **78** 3769
[5] Lee W II, Shelton R N, Dhar S K and Gschneidner Jr K A 1987 *Phys. Rev.* B **35** 8523
[6] Gignoux D and Gomez-Sal J C 1984 *Phys. Rev.* B **30** 3967
[7] Lacroix C and Cyrot M 1979 *Phys. Rev.* B **20** 1969
[8] Tsunetsugu H, Sigrist M and Ueda K 1993 *Phys. Rev.* B **47** 8345
[9] Hamada M and Shimahara H 1995 *Phys. Rev.* B **51** 3027
[10] Jarrell M, Pang H and Cox D L 1997 *Phys. Rev. Lett.* **78** 1996
[11] Kikoin K A, Kiselev M N and Mishchenko A S 1994 *JETP Lett.* **60** 600
[12] Continentino M A, Japiassu G M and Troper A 1989 *Phys. Rev.* B **39** 9734
[13] Miranda E, Dobrosavljevic V and Kotliar G 1997 *Phys. Rev. Lett.* **78** 290
[14] Castro Neto A H and Jones B A 2000 *Phys. Rev.* B **62** 14975
[15] Rappoport T G, Saguia A, Boechat B and Continentino M A *Phys. Rev.* B at press
[16] Jullien R, Fields J N and Doniach S 1977 *Phys. Rev.* B **16** 4889
[17] Scalettar R T, Scalapino D J and Sugar R J 1985 *Phys. Rev.* B **31** 7316
[18] Santini P and Sólyom J 1992 *Phys. Rev.* B **46** 7422
[19] Moukouri S, Caron L G, Bourbonnais C and Hubert L 1995 *Phys. Rev.* B **51** 15920
[20] Zhang G M, Gu Q and Yu L 2000 *Phys. Rev.* B **62** 69
[21] Indekeu J O, Maritan A and Stella A L 1982 *J. Phys.* A **15** L291
[22] Plascak J A, Figueiredo W and Grandi B C S 1999 *Bras. J. Phys.* **29** 579
[23] Granato E and Continentino M A 1993 *Phys. Rev.* B **48** 15977
[24] Schrieffer J R and Wolff P A 1966 *Phys. Rev.* **149** 491
[25] Droz M, Maritan A and Stella A L 1982 *Phys. Lett.* A **92** 287
[26] Plascak J A 1984 *J. Phys. A: Math. Gen.* **17** L279
[27] Godart C, Gupta L C, Tomy C V, Thompson J D and Vijayaraghavan R 1989 *Europhys. Lett.* **8** 375
[28] Schröder A *et al* 2000 *Nature* **407** 351
[29] Endstra T, Nieuwenhuys G J and Mydosh J A 1993 *Phys. Rev.* B **48** 9595
[30] Das I and Sampathkumaran V 1991 *Phys. Rev.* B **44** 9711
[31] Dakin S, Rapson G and Rainford B D 1992 *J. Magn. Magn. Mater.* **108** 117
[32] Godart C, Gupta L C, Tomy C V, Thompson J D and Vijayaraghavan R 1989 *Europhys. Lett.* **8** 375
[33] Cornelius A L and Schilling J S 1994 *Phys. Rev.* B **49** 3955
[34] Assad F F 1999 *Phys. Rev. Lett.* **83** 796